Vol 17 No 12, December 2008
1674-1056/2008/17(12)/4665-04

Chinese Physics B

© 2008 Chin. Phys. Soc.
and IOP Publishing Ltd

Synthesis of industrial diamonds using FeNi alloy powder as catalyst

Zhou Lin(周　林)[a)b)], Jia Xiao-Peng(贾晓鹏)[a)c)], Ma Hong-An(马红安)[a)c)†], Zheng You-Jin(郑友进)[a)], and Li Yan-Tao(李彦涛)[a)]

[a)] *National Laboratory of Superhard Materials, Jilin University, Changchun* 130012, *China*
[b)] *Department of Physics, Heilongjiang University, Harbin* 150080, *China*
[c)] *Henan Polytechnic University, Jiaozuo* 454000, *China*

(Received 4 May 2008; revised manuscript received 4 June 2008)

Synthesis of diamond single crystals in $Fe_{80}Ni_{20}$–C system was carried out in a cubic anvil high-pressure and high-temperature apparatus. This paper reports that the surface morphology and inclusion distribution of the grown diamonds had been observed. It finds that the inclusions in cubic and octahedral diamonds radiated along certain crystal orientation, while the inclusion distribution in cubo-octahedral diamond seemed independent of crystal orientation. By using scanning electron microscope, the surface morphology of the three shapes of diamonds was observed. The results of Mossbauer spectrum indicated that there were iron-inclusions Fe_3C and Fe–Ni alloy in the diamonds. According to the Fe–C phase diagram, Fe_3C should have formed during the quenching process. Nickel might have an inhibitory effect on the formation of Fe_3C.

Keywords: $Fe_{80}Ni_{20}$, diamond, inclusion, morphology
PACC: 8110D

1. Introduction

Diamond is a kind of representative superhard material with many unsurpassed physical and chemical properties. As a familiar impurity defect in diamond, inclusions can strongly influence the physical properties of diamond, including mechanical, electric, optical and thermal properties. For high pressure and high temperature (HPHT) grown diamond, the composition of inclusions usually corresponds to pure metal, alloy or compounds. The formation and distribution of inclusions usually depend on the growth conditions. Some data on the spatial distribution of various impurities in synthetic diamonds have been obtained.[1−4] Wakatsuki [5] gave a distribution rule, classified in five cases covering all shapes of particles consisting of two main, {111} and {100} facets. Kanda *et al*[6] who used $Fe_{50}Ni_{25}Co_{25}$ alloy as solvent metal and synthesized diamond crystal at the interface of the graphite and solvent metal layer, found that the bands of inclusions extended only to the corners or edges on the graphite side.

Morphology is another important index for diamond. Diamonds with different morphology may have different properties to be used in corresponding areas. The morphology of the diamonds grown in molten metals under HPHT has been investigated by many authors recently.[7−10]

This paper reports that diamonds are synthesized by film growth method using $Fe_{80}Ni_{20}$ alloy powder as catalyst. The inclusions in diamonds have been investigated from several aspects such as spatial distribution, composition and contributing factor. This work might contribute to the further study on the mechanism of inclusion formation.

2. Experimental details

Diamond synthesis was carried out in a cubic anvil HPHT apparatus (SPD-6×1670) at temperatures 1700–1800 K and pressures 5.7 GPa for 12 min. The pressure was estimated based on the pressure-induced phase transitions of bismuth, thallium and barium. And the temperature was measured using a Pt6%R-Pt30%Rh thermocouple.[11]

The experimental raw materials are $Fe_{80}Ni_{20}$ alloy powder and natural crystalline flake graphite powder, both of them are 200 mesh in granularity and higher than 99.9% in purity. The mixture of graphite and alloy was uniformly mixed according to fixed mass ratios of 6:4. Then it was shaped into disc form to fit in the high pressure sample assembly (Fig.1).

†Corresponding author. E-mail: maha@jlu.edu.cn

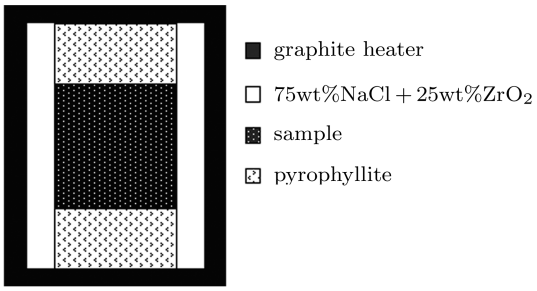


Fig.1. Sample assembly sketch of high pressure experiment.

After synthesis under HPHT, the collected samples were placed in the boiling mixture of H_2SO_4 and HNO_3 to extract diamond grits from the massive experimental samples. And then physical optical microscope and scanning electron microscope (SEM) (LINK-ISIS JSM5310) were applied for observation. The inclusions in diamond crystals were characterized on an OXFORD MS-500 transmission Mossbauer spectroscopy at room temperature. The spectra were recorded using a ^{57}Co/Pd source.

3. Results and discussions

3.1. Crystal shape and inclusion distribution

Diamond single crystals with cubic, cubo-octahedral and octahedral shape were respectively synthesized under different conditions. Then the inclusion distribution of diamonds was observed under an optical microscope by properly adjusting the intensity and incidence angle of background light. Figure 2 shows the crystal photos and inclusion distribution diagrammatic sketch. The experimental conditions and observation results are presented in Table 1.

It is worth while mentioning that in the cubo-octahedral diamond grits, there are little inclusions and the distribution of inclusions seems independent of any crystal orientation. The results are different from those in the literature,[5] which also gives the distribution rule in cubo-octahedral grits, inclusions are distributed on sectorial planes defined by the nuclear site and crystal edges where two facets of the same kind of crystallographic index ⟨100 or 111⟩ meet together.

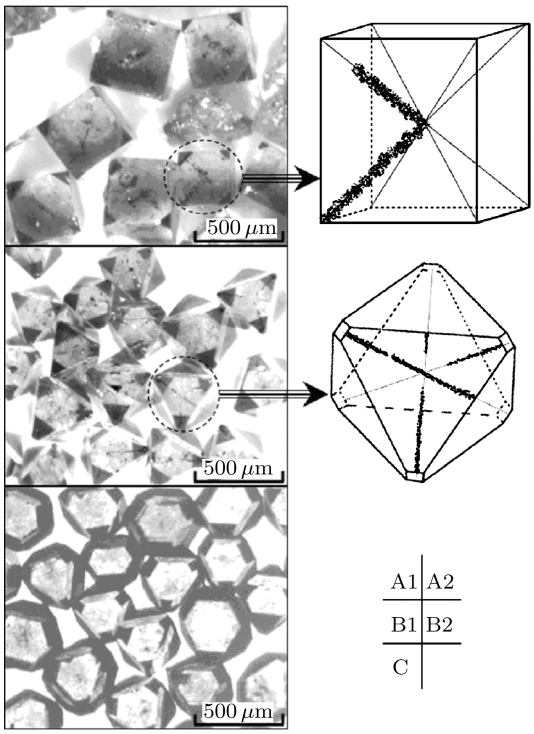


Fig.2. Crystal photos and inclusion distribution diagrammatic sketch.

Table 1. Experimental conditions and observation results.

P/GPa	T/K	Crystal shape	Inclusion distribution
5.7	1700	cubic	radiate along ⟨111⟩ orientation
5.7	1750	cubo-octahedral	independent of crystal orientation
5.7	1800	octahedral	radiate along ⟨100⟩ orientation

3.2. Surface morphology of diamond crystals

Figure 3 shows the SEM photographs of diamond crystals. As can be seen from the photos, the surface of cubic and octahedral diamond is flat except for some different tiny growth striations. The {100} faces of cubic diamond exhibit unorderly dendritic patterns, while the {111} faces of the octahedral exhibit orderly imbricate patterns. Both the {111} and {100} faces of cubo-octahedral diamonds are rough. Its {100} faces exhibit terraced striations with space between about 10 μm. Some local regions of its {111} faces exhibit

dense curvilinear patterns.

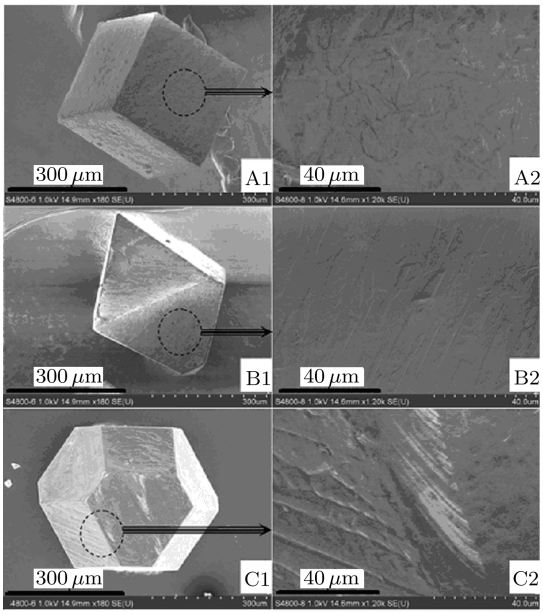


Fig.3. SEM photographs of diamond crystals.

3.3. Composition of inclusions

After a series of thorough acid treatment and cleaning, the collected diamond samples were crushed into 200 mesh powder. And then the transmission Mossbauer spectroscopy measurement was carried out.

In order to explore the rules of inclusion formation, diamonds grown in $Fe_{90}Ni_{10}$-C system were used as comparison. The transmission Mossbauer spectra of the diamonds are shown in Fig.4. The results

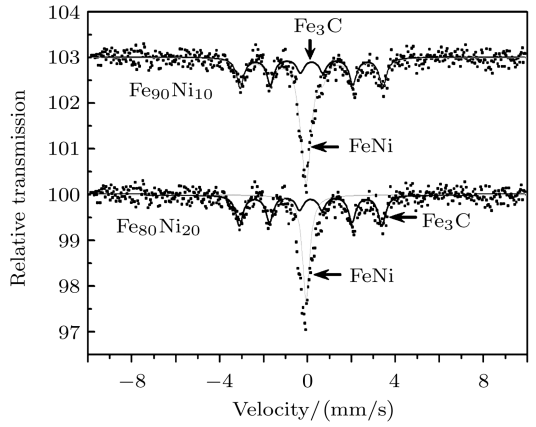


Fig.4. Transmission Mossbauer spectrum of synthetic diamonds.

indicate that inclusions in the diamonds grown in the two systems are all composed of Fe_3C and Fe-Ni alloy, only their relative contents are different (Table 2). With the increase of Ni content in catalyst, the Fe_3C content tends to decrease.

Table 2. Relative content of Fe_3C and Fe-Ni inclusion in diamonds.

Catalyst for synthesis	iron-inclusion of diamonds	
	Fe_3C content	Fe-Ni alloy content
Fe_{90} Ni_{10}	46.8%	53.2%
Fe_{80} Ni_{20}	40.1%	59.9%

3.4. Formation mechanism of inclusion

The diamond growth process involves an equilibrium between the diffusing away of impurities and the absorption of incoming flux. The formation of inclusions has a relation with the crystal growth rate. Once the growth rate on certain crystal orientation is higher, the impurities would be more easily trapped in the corresponding area. So the inclusions in cubic and octahedral diamonds usually distribute on the bands connecting the nuclear site with the corners.

For cubo-octahedral diamonds, there are little differences among the growth rates in all orientations, only the growth rates of crystal edges are relatively higher. So there are usually more inclusions in the sectorial planes defined by the nuclear site and crystal edges. However, in our present research, the global growth rate of the cubo-octahedral diamonds is relatively lower, so that there are little inclusions in the crystals, and the distribution of inclusions seems independent of any crystal orientation under optical microscope.

In the Fe-C binary system (Fig.5), Fe_3C is stable to 1688 K, preventing diamond growth below this temperature.[12] Crystallization will take place at temperatures a little above this temperature. During the synthesis, a small quantity of melting Fe-Ni alloy and the dissolved carbon would be trapped in the crystal. While quenching after synthesis, the P-T conditions enter into the stable region of Fe_3C, so that some iron in Fe-Ni alloy reacts with the dissolved carbon, and Fe_3C comes into being. Thus the iron-inclusions in diamonds include both Fe_3C and the remnant Fe-Ni alloy.

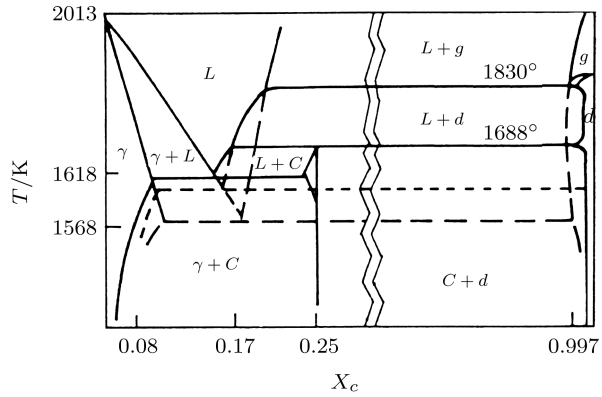


Fig.5. Fe-C binary system at 5.7 GPa.[12].

Nickel is a metal with very strong chemical activity. Based on the above results, we infer that Ni had inhibited the formation of Fe_3C during the quenching process, to a certain extent. And with the increase of Ni content, this inhibitory effect becomes stronger and stronger, leading to the decrease of Fe_3C relative content in iron-inclusions.

4. Conclusions

Industrial diamonds were successfully synthesized in FeNi–C system. The inclusions in cubic and octahedral diamonds radiated along certain crystal orientation, while the inclusion distribution in cubo-octahedral diamond seemed independent of any crystal orientation. The surface morphology of diamond varied with the crystal shape. There were two kinds of iron-inclusions Fe_3C and Fe-Ni alloy in the grown diamonds. With the increase of Ni content in catalyst, the relative content of Fe_3C tended to decrease.

References

[1] Jia X, Hayakawa S, Li W, Gohshi Y and Wakatsuki M 1999 *Diamond Relat. Mater.* **8** 1895
[2] Burns R C, Cvetkovic V, Dodge C N, Evans D J F, Rooney M L T, Spear P M and Welbourne C M 1990 *J. Cryst. Growth* **104** 257
[3] Yelisseyev A, Nadolinny V, Feigelson B, Terentyev S and Nosuk-hin S 1996 *Diamond Relat. Mater.* **5** 1113
[4] Kanda H and Watanabe K 1997 *Diamond Relat. Mater.* **6** 708
[5] Wakatsuki M 1984 *Materials Science of The Earth's Interior* (Tokyo:Terra Scientific Publishing Company) p351
[6] Kanda H, Setaka N, Ohsawa T and Fukunaga O 1981 *J. Crystal Growth* **51** 629
[7] Pal'yanov Yu, Kupriyanov I, Khokhryakov A, Borzdov Yu, Gusev V and Royen J Van 2003 *Diamond Relat. Mater.* **12** 1510
[8] Zhou L, Jia X P, Ma H A, Chen L X, Guo W L and Li Y T 2006 *Diamond Relat. Mater.* **15** 1318
[9] Zhang J Q, Ma H A, Jiang Y P, Liang Z Z, Tian Y and Jia X 2007 *Diamond Relat. Mater.* **16** 283
[10] Kanda H, Akaishi M, Setaka N, Yamaoka S and Fukunaga O 1980 *J. Mater. Sci.* **15** 2743
[11] Ma H A, Jia X P, Chen L X, Zhu P W, Guo W L, Guo X B, Wang Y D, Li S Q, Zou G T, Zhang G and Bex P 2002 *J. Phys. Condens. Matter* **14** 11269
[12] Strong H M and Chrenko R M 1971 *J. Phys. Chem.* **75** 1838